JOURNAL OF SOLID STATE CHEMISTRY 84, 1–9 (1990)

High-Pressure Synthesis of Cubic Perovskite $CaLaMgMnO_{5.5+x}$

JIN-HO CHOY, GERARD DEMAZEAU,* AND JEAN MICHEL DANCE*

*Department of Chemistry, Seoul National University, Seoul 151, Korea, and *Laboratoire de Chimie du Solide du CNRS, Universite de Bordeaux I, 33405 Talence Cedex, France*

Received May 24, 1989; in revised form August 2, 1989

Oxygen-deficient perovskite $CaLaMgMn^{IV}_{1-x}Mn^{VI}_xO_{5.5+x}$ (indicated by *P*) has been prepared at 930°C for 10 mn using high oxygen pressure (60 kbar). X-ray diffraction study indicates that *P* has a simple cubic unit cell (a = 3.923 Å). The average oxidation state of Mn in *P* was determined by redox titration before (4.13) and after (4.03) thermal treatments at 300, 900, and 1100°C and was confirmed by thermogravimetry analysis. Two paramagnetic configurations are observed from the EPR spectrum: One isotropic signal characterized by g = 1.994, ΔH = 950 G, and an anisotropic signal with $g_\perp$ = 1.978, $g_\parallel$ = 1.938. They correspond respectively to octahedrally coordinated Mn(IV) and to tetrahedrally coordinated Mn(VI). According to magnetic susceptibility measurements, the constant spin-only moment observed between 77 and 650 K (μ_{eff} = 3.8 μ_B) is consistent with a Mn(IV)—$^4A_{2g}$ ground term—(μ_{eff} = 3.87 μ_B). Such behavior can be explained by the low Mn(VI) content in *P*.

Introduction

The +IV oxidation state of manganese is frequently found in the oxygen lattices with octahedral coordination. Improved methods of preparation and characterization allow one to report the stabilization of Mn(IV) in the ternary oxide system $AMnO_3$ (A = alkalimetal ion) (*1–4*), in some quaternary oxides such as $ATi_{1-x}Mn_xO_3$, $AZr_{1-x}Mn_xO_3$, and so on (*5*).

We have recently described a new Mn(IV) oxide ($Sr_{0.5}La_{1.5}Li_{0.5}Mn_{0.5}O_4$) with a structure derived from K_2NiF_4, where the Mn(IV) ions are isolated from each other (*6*). In order to stabilize and characterize the manganese with an oxidation state higher than +IV we have proposed to prepare the ALaMgMnO$_6$-ordered perovskites. This paper describes the synthesis and the study of the oxygen-deficient perovskite $(CaLa)(MgMn^{IV}_{1-x}Mn^{IV+n}_x)O_{5.5+nx/2}$.

Experimental

As starting materials, reagent-grade high-purity calcium, lanthanum, magnesium, and manganese nitrates were used. These materials mixed in stoichiometric ratio were first calcinated at 700°C in order to decompose the nitrates. In a second step the remaining product was treated 10 hr at 850°C. The third step consisted of a five-day heating under oxygen atmosphere (P_{O_2} = 1 bar) at 900°C. Since high pressure favors an increase in coordination number (4 to 6) and oxygen pressure enhances stabili-

0022-4596/90 $3.00

TABLE I

AVERAGE OXIDATION STATE OF MANGANESE DETERMINED BY REDOX TITRATION

Conditions in final heat treatment of $(CaLa)(MaMn)O_{5.5+x}$	Oxidation state (±0.05)
(I): After 60 kbar/930°C	4.13
(II): (I) was reheated at 300°C in air	4.03
(III): (I) was reheated at 900°C in air	4.04
(IV): (I) was reheated at 1100°C in N_2	4.03

zation of Mn oxidation states higher than IV, the final treatment was made under high-pressure and high-temperature conditions using a belt-type apparatus (*7*) in a sealed gold tube. High oxygen pressure was generated *in situ* by thermal decomposition of additional $KClO_3$ (*7*). After the reaction the remaining KCl was leached out rapidly with distilled water and ethanol.

The oxidation state of manganese was determined by redox titration after dissolution in a HCl solution and the evolved free iodine was titrated by sodium thiosulfate. Experimental results are given in Table I. Variation in the oxidation state of manganese was also followed by thermogravimetric analysis.

X-ray diffraction analysis was carried out using a Debye–Scherrer camera with a radius of r = 114.8 mm, a Phillips–Norelco diffractometer using Ni-filtered Cu$K\alpha$ radiation, and a Guinier photographic method (λ = 1.5418 Å). The lattice parameters were refined from the powder data by a least-squares method. The thermal evolution of the lattice parameters during the thermogravimetric analysis was also checked by high-temperature X-ray powder diffraction.

In order to estimate the oxidation state of paramagnetic manganese ions, the magnetic susceptibility was measured with a Faraday balance between 77 and 650 K and the EPR spectra were obtained in a temperature range 10–300 K using a Bruker-ER 200 tt X-band spectrometer associated with an Oxford instruments cryostat.

Results and Discussion

The final high oxygen pressure treatment (60 kbar, 930°C, 10 mn) leads reproducibily to a single perovskite phase. No diffraction lines other than those attributable to the cubic perovskite structure of ABO_3 were found in the X-ray powder pattern. The absence of such extra lines indicates that no superstructure can be involved and suggests that Mg and Mn ions are probably distributed randomly in the oxygen perovskite lattice. For all the similar perovskites with the formula (CaLa) $(BB')O_6$, where B(II) B'(V) = (MgMo), (MgTa), (MgRu), (MgIr), (CaTa), (MnMo), (MnTa), and (MnTi), reported previously in the literature (*8–12*), the superlattice lines (induced by an ordered arrangement of B and B' ions in the oxygen–octahedral sites) were detected in the X-ray diffraction patterns (Table II). The unit cell parameter of (CaLa)(MgMn) $O_{5.5+x}$ prepared in this study was found close to 3.823 Å. In Fig. 1, the average parameter $\bar{a}$ (Table II), defined as the cube root of the cell volume of the perovskite unit, was plotted against the mean ionic radius $\bar{r} = (1/2)(r_B + r_{B'})$. The ionic radii used in this plot are from Shannon (*13*). They agree well with a linear relationship $\bar{a} = f(\bar{r})$ except with the disordered (MgMn) pair. Such a deviation could be attributed to a larger average value of the ionic radius of manganese ions. This phenomenon would be induced by the stabilization of a large percentage of Mn(IV).

According to the redox titration of the high-pressure treated sample, the average valency state of manganese was estimated to be 4.13, which confirms that a large part of manganese stabilized in the perovskite $(CaLa)(MgMn)O_{5.5+x}$ has a lower oxidation state than V+. For this reason such a perovskite can be written as (CaLa)

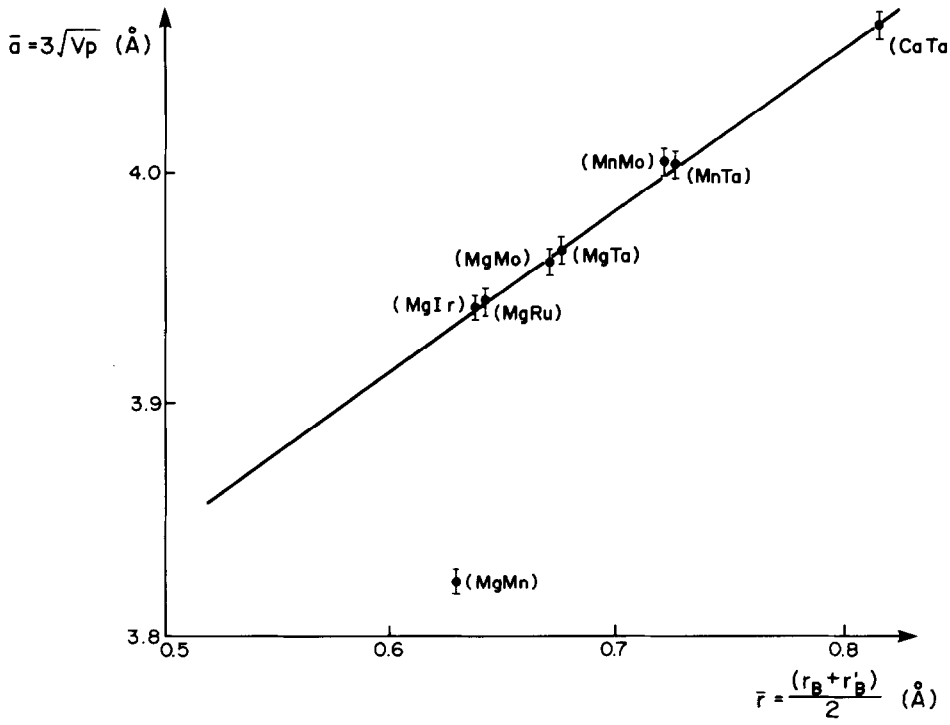

FIG. 1. The linear relation between cube root of cell volume versus mean ionic radius of (BB') ions for perovskites $CaLa(BB')O_6$.

TABLE II

LATTICE CONSTANTS AND PEROVSKITE PARAMETER $\bar{a} = 3\sqrt{Vp}$ OF PEROVSKITE-TYPE COMPOUNDS $(CaLa)(BB')O_6$ USED IN THIS WORK

	Lattice parameter				
(BB')	a(Å)	b(Å)	c(Å)	$\bar{a}$(Å)	Remarks
MgMn	3.823	—	—	3.823	This work $(Mg^{II}, Mn^{IV}_{0.93}Mn^{VI}_{0.07})$ Disordered
MgMo	5.551(a)	5.622(1)	7.875(1)	3.959	(Mg^{II}, Mo^{V}) Ordered
MgTa	5.558(3)	5.633(3)	7.901(2)	3.966	(Mg^{II}, Ta^{V})
MgRu	5.513	5.544	7.89(9)	3.941	(Mg^{II}, Ru^{V})
MgIr	5.533	5.573	7.83(9)	3.943	(Mg^{II}, Ir^{V})
CaTa	5.654	5.890	8.164	4.061	(Ca^{II}, Ta^{V})
MnMo	5.596(2)	5.766(2)	7.976(1)	4.005	(Mn^{II}, Mo^{V})
MnTa	5.597(4)	5.741(4)	7.994(2)	4.003	(Mn^{II}, Ta^{V})
MnTi	3.912 (α = 90°12R)				(Mn^{III}, Ti^{IV})

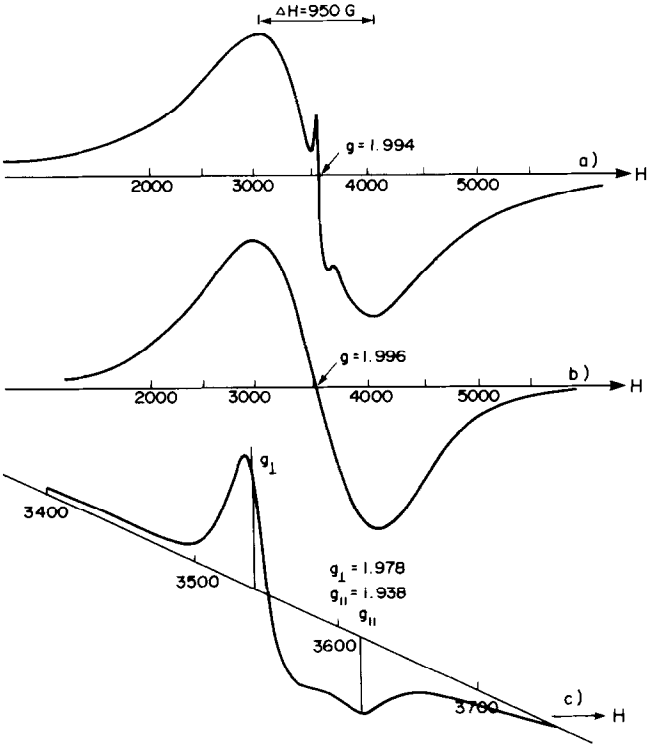

FIG. 2. EPR spectra of $CaLaMgMn^{IV}_{0.93}Mn^{VI}_{0.07}O_{5.57}$ at 300 K (a) immediately after high-pressure experiment; (b) heated sample of (a) at 300°C in air; and (c) enlarged spectrum of weak peak in (a) which disappeared after heat treatment at 300°C (as shown in (b)).

$(MgMn)O_{5.5+x}$. Two kinds of oxidation state equilibria can be proposed: $CaLaMgMn^{IV}_{1-x}Mn^{V}_{x}O_{5.5+x/2}$ or $CaLaMn^{IV}_{1-x}Mn^{VI}_{x}O_{5.5+x}$. Due to the existence of oxygen vacancies inducing either tetrahedral sites (T_d) or square pyramidal sites (C_{4v}), Mn(V) (d^2) or Mn(VI) (d^1) could be stabilized in such a lattice. EPR and magnetic susceptibility measurements are used for selecting the appropriate composition and oxidation state. The EPR spectra at room temperature indicated two kinds of paramagnetic species (Fig. 2). The upper spectrum (a) was recorded directly after quenching the product under high pressure. In the middle of the intense and broad signal (ΔH = 950 G) with g = 1.994, a weaker additional sharp anisotropic signal was observed. The g values of this signal were estimated as $g_\perp \cong 1.978$ and $g_\parallel \cong 1.938$, respectively, from the enlarged spectrum (c). This weak signal disappeared upon reheating at 300°C in air as shown in spectrum (b). The $g_{exp.}$ of the main peak is actually not changed after heating (g = 1.996). This observed g value of 1.995 ± 0.01 is very close to those of Mn(IV) in $SrTiO_3$ (g = 1.994 ± 0.001) (*14, 15*), Mn(IV) in calcium zirconate (g = 1.994) (*16*), Mn(IV) in α-Al_2O_3 (g = 1.994) (*17*), and Mn(IV) in $Sr_{0.5}La_{1.5}Li_{0.5}Mn_{0.5}O_4$ (g = 1.995 ± 0.001) (*6*). The isotropic $g_{calc.}$ factor was calculated for octahedral Mn(IV) by the equation

$$g = g_e - \frac{8k^2\lambda}{\Delta}.$$

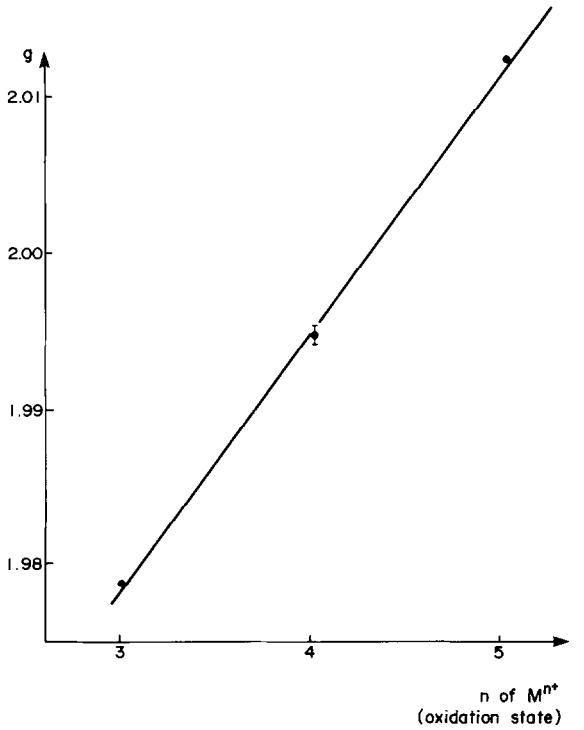

FIG. 3. Variation of Lande g factor versus the oxidation state in the isoelectronic ion series (Cr^{III}, Mn^{IV}, and Fe^{V} are considered).

The spin-orbit coupling constant (λ) used was 138 cm^{-1} (*18*) and the octahedral ligand field splitting (Δ) was 22.000 cm^{-1} (*19*). If we admit k^2 close to 0.6, $g_{calc.}$ (1.998) is in agreement with the observed g value (g = 1.995) (*2*). The $g_{exp.}$ values of the isoelectronic cations Cr(III) (*21*), Mn(IV) (*6*), and Fe(V) (*22, 23*) observed in octahedral environments are plotted versus the oxidation states (Fig. 3). The g-factors show a progressive increase, which has been ascribed to an increasing contribution of covalent bonding along the series. The weak signal (c), which disappeared upon heating, should be attributed to the Mn(VI) ($3d^1$) stabilized in a pseudo-tetrahedral site. This interpretation is most probably due to the anisotropic nature of the EPR signal. As shown in Fig. 4 an octahedral site can be transformed into a tetrahedral site through a displacement of Mn along the |110| direction and the creation of two oxygen vacancies. The EPR spectrum of Mn(VI) in K_2CrO_4 at 20 K shows an anisotropic signal (g_x = 1.970 ± 0.005, g_y = 1.966 ± 0.001, g_z = 1.938 ± 0.01 (*24*), which is quite consistent with our observation. The weak signal could have been attributed to Mn(V) ($3d^2$) but in an octahedral environment such an EPR signal cannot be observed at 300 K but only below 4 K. On the other hand Mn(V) in a tetrahedral site can be easily detected by EPR at room temperature but with a higher g value (g = 2.02 ± 0.01) (*21*). The experimental results of redox titration ($Mn^{4.13}$) and EPR study (existence of Mn(VI)) suggest, therefore, the formulation of the composition of the high-pressure sample as $CaLaMgMn^{(IV)}_{0.93}Mn^{(VI)}_{0.07}O_{5.57}$.

In order to confirm the reductive behav-

TABLE III

X-RAY POWDER DIFFRACTION DATA FOR $CaLaMgMn^{IV}_{1-x}Mn^{VI}_{x}O_{5.5+x}$ ($x = 0.07$)

$h\ k\ l$	I/I_0	d_0(Å)	d_c(Å)
1 0 0	23	3.767	3.823
1 1 0	100	2.692	2.703
1 1 1	18	2.199	2.207
2 0 0	31	1.905	1.912
2 1 0	5	1.708	1.710
2 1 1	18	1.560	1.561
2 2 0	10	1.351	1.352
3 0 0	1	1.276	1.274
3 1 0	6	1.210	1.209
3 1 1	2	1.153	1.153

$\bar{a} = 3.823(2)$

ior at high temperature as shown in Table I and Fig. 2, oxygen nonstoichiometry has been systematically studied by thermogravimetry together with the high-temperature X-ray analysis. Three distinct domains of nonstoichiometry were observed within the temperature range 20–550°C. As shown in Fig. 5, plateau III, formed above 300°C, is at first assumed to be the result of the formation of $CaLaMgMnO_{5.5} + (x/2)O_2$. Plateau II, whose stability temperature domain is very narrow (110–130°C), can be formulated as follows by considering the slight mass loss between II and III:

$$CaLaMgMn^{(IV)}_{0.93}Mn^{(VI)}_{0.07}O_{5.57}(II) \rightarrow CaLaMgMn(IV)O_{5.5} + 0.035O_2(III).$$

The average oxidation state of Mn from TG analysis was calculated as 4.14, which is in good agreement with the value 4.13 obtained from chemical titration.

The difference of mass between I and II might be due to the desorption of H_2O adsorbed on the fine particle surface. In order to confirm this unexpected effect of H_2O, a heat treatment at 60°C under vacuum (10^{-3} Torr) has been carried out for 3 hr. The

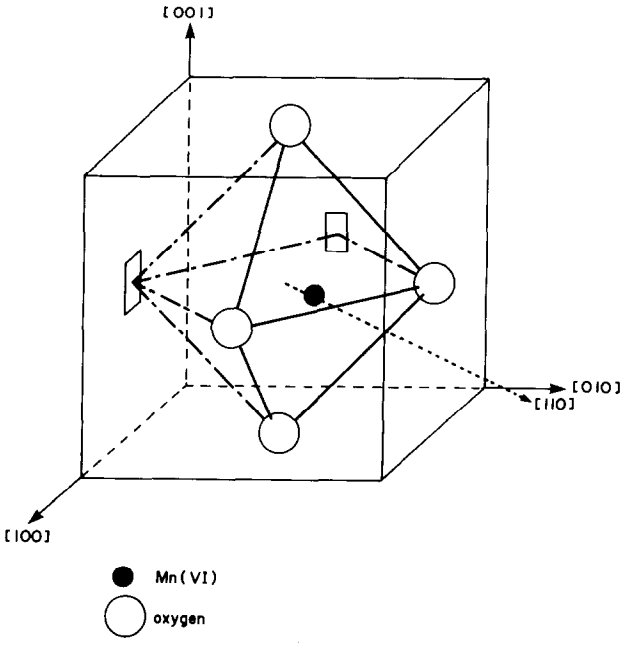

FIG. 4. Transformation of an octahedral site with oxygen *cis*-vacancies to a tetrahedral site through a displacement of Mn^{VI} along a [110] direction.

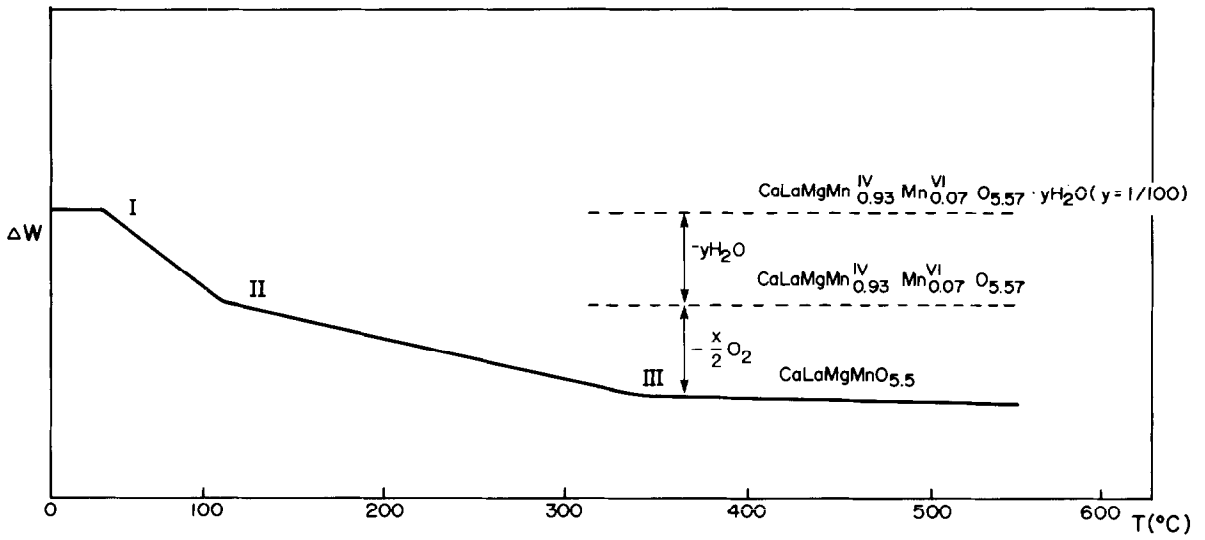

FIG. 5. Oxygen stoichiometry of $CaLaMgMn^{IV}_{1-x}Mn^{VI}_{x}O_{5.5+x}$ as a function of heat-treatment temperature.

average content of H_2O loss was found to be approximately 1/100 mole of H_2O per mole of $CaLaMgMn^{IV}_{0.93}Mn^{VI}_{0.07}O_{5.57}$. Such a result is quite consistent with the mass loss between I and II.

The temperature domain, where the oxygen removal from the lattice seems to be significant, was examined by high-temperature X-ray diffraction analysis in order to check some structural transition due to oxygen deficiency. No structural transition was found, only a positive elongation was observed from 20°C up to 700°C with a coefficient close to $3 \cdot 10^{-5}$ Å/°C.

The magnetic susceptibility of $CaLaMgMn^{IV}_{0.93}Mn^{VI}_{0.07}O_{5.57}$ has been measured between 77 and 650 K. After correction for diamagnetic contribution, the variation of χ_M^{-1} vs T appears to fit with the Curie–Weiss law for $120 < T < 650$ K (Fig. 6). Such a result would be controversial with the thermogravimetric curve characterizing a change in the oxidation state for manganese in the same temperature range. However, the constant magnetic moment ($\cong 3.8\ \mu_B$) close to the spin-only value for Mn(IV) could be due to the small Mn(VI) content (close to 7%) corresponding to the error limit of the magnetic susceptibility measurements.

The strength of the Mn–O bond is dependent upon both size and basicity of the A cation in perovskite $(A\text{La})(\text{MgMn})O_{5.5+x'}$, where A corresponds to Ca, Sr, and Ba. If the A cation becomes more acidic (Ba → Sr → Ca), then the ionicity of the Mn–O bond increases, making the σ(Mn–O) bond weaker. On the other hand, the π(Mn–O) bond competing with the $\sigma(A\text{–O})$ bond becomes stronger with a destabilization of π^*(Mn–O). Consequently the local crystal field energy (the energy difference between σ_g^* and π^*) is enhanced gradually from Ba to Ca (Fig. 7). Therefore Ca compound compared to Ba or Sr compounds favors oxygen vacancies, which stabilize the smallest cation by a reduction in coordination number. From the increase in the local crystal field and the size reduction in Ca compound, it could be possible to explain the presence of a small amount of Mn(VI).

Conclusions

The $CaLaMgMnO_{5.5+x}$ oxide with the cubic perovskite structure has been prepared

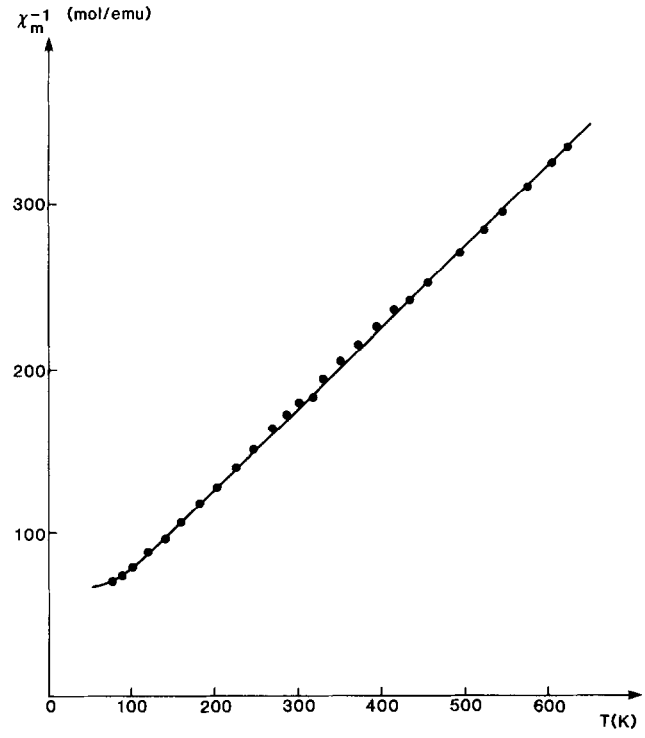

FIG. 6. Reciprocal molar magnetic susceptibility versus absolute temperature for CaLaMg $Mn^{IV}_{0.93}Mn^{VI}_{0.07}O_{5.57}$.

under high pressure. Through EPR study, Mn(VI) in a tetrahedral site and Mn(IV) in an octahedral site have been detected. The corresponding composition can be written as $CaLaMgMn^{IV}_{0.93}Mn^{VI}_{0.07}O_{5.57}$. The stabilization of small amounts of manganese VI in such a lattice could be induced by the large number of oxygen vacancies favoring tetra-

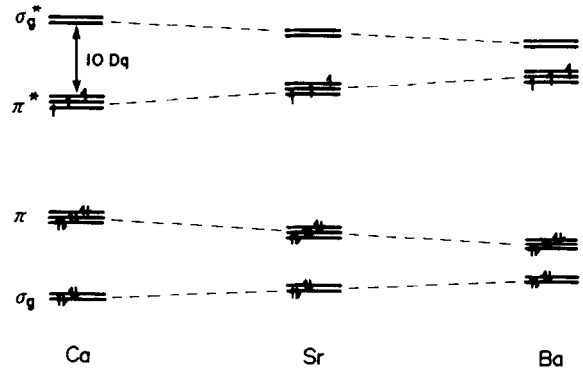

FIG. 7. Idealized MO diagrams of MnO_6 octahedron in $(A\text{La})(\text{MgMn})O_6$ with A = Ca, Sr, and Ba. Note that the local crystal field energy (10 Dq) becomes greater from Ba to Ca.

hedral sites and the strong cyrstal field energy at the manganese site due to competing σ and π bonding.

References

1. F. GALASSO, "Structure, Properties and Preparation of Perovskite-Type Compounds," Pergamon Press, Oxford (1969).
2. J. B. MACCHESNEY, N. J. WILLIAMS, J. F. POTER, AND R. C. SHERWOOD, *Phys. Rev.* **164,** 779 (1967).
3. W. M. YUDIN, A. I. GAURALISHIMA, M. V. ARTMEVA, AND M. F. BRYZKINA, *Fiz. Tverd. Tela. (Leningrad)* **7,** 2292 (1965).
4. T. TAKEDA AND S. OHARA, *J. Phys. Soc. Japan* **35,** 275 (1974).
5. M. ARJOMAND AND D. J. MACHIN, *J. Less-Common Met.* **61,** 133 (1978).
6. E. KIM, G. DEMAZEAU, J. M. DANCE, M. POUCHARD, AND P. HAGENMULLER, *C. R. Seances Acad. Sci. Ser. 2* **16,** 491 (1985).
7. G. DEMAZEAU, *Actual. Chim.*, 46 (1985).
8. T. NAKAMURA AND J. H. CHOY, *J. Solid State Chem.* **20,** 3, 233 (1977).
9. M. WALEWSKI, B. BUFFAT, G. DEMAZEAU, F. WAGNER, M. POUCHARD, AND P. HAGENMULLER, *Mater. Res. Bull.* **18,** 881 (1983).
10. M. WALEWSKI, Thesis, Univ. Bordeaux I (1982).
11. J. B. GOODENOUGH, "Magnetism and the Chemical Bond," Interscience, New York (1963).
12. F. GALASSO AND J. PYLE, *Inorg. Chem.* **2,** 482 (1963).
13. R. D. SHANNON, *Acta Crystallogr. A* **32,** 751 (1976).
14. K. A. MÜLLER, *Helv. Phys. Acta* **33,** 497 (1960).
15. K. A. MÜLLER, *Phys. Rev. Lett.* **2,** 341 (1959).
16. B. HENDERSON, *Proc. Phys. Soc.* **92,** 1064 (1967).
17. S. GESCHWIND, R. KISLIUK, M. P. KLEIN, J. P. REMEIKA, AND D. L. WOOD, *Phys. Rev.* **126,** 1684 (1962).
18. F. E. MABBS AND D. J. MACHIN, Eds., "Magnetism in Transition Metal Complexes," Chapman & Hall, London (1973).
19. J. C. BOULOUX, J. L. SOUBEYROUX, G. LE FLEM, AND P. HAGENMULLER, *J. Solid State Chem.* **38,** 34 (1981).
20. J. E. WERTZ AND J. R. BOLTON, "Electron Spin Resonance; Elementary Theory and Practical Application," McGraw–Hill, New York (1972).
21. G. W. LUDWIG AND H. H. WOODBURY, *in* "Solid State Physics" (F. Seitz and D. Turnbull, Eds.), Vol. 1, Academic Press, New York (1962).
22. B. N. FIGGIS, "Introduction to Ligand Fields," Interscience, New York (1967).
23. G. DEMAZEAU, B BUFFAT, F. MENIL, L. FOURNES, M. POUCHARD, J. M. DANCE, P. FABRITCHNYI, AND P. HAGENMULLER, *Mater. Res. Bull.* **16,** 1465 (1981).
24. A. CARRINGTON, D. J. E. INGRAM, AND K. A. K. LOTT, *Proc. R. Soc. London A* **254,** 101 (1960).